

Occ-LLM: Enhancing Autonomous Driving with Occupancy-Based Large Language Models

Tianshuo Xu¹, Hao Lu¹, Xu Yan², Yingjie Cai², Bingbing Liu² and Yingcong Chen^{1*}

Abstract—Large Language Models (LLMs) have made substantial advancements in the field of robotic and autonomous driving. This study presents the first Occupancy-based Large Language Model (Occ-LLM), which represents a pioneering effort to integrate LLMs with an important representation. To effectively encode occupancy as input for the LLM and address the category imbalances associated with occupancy, we propose Motion Separation Variational Autoencoder (MS-VAE). This innovative approach utilizes prior knowledge to distinguish dynamic objects from static scenes before inputting them into a tailored Variational Autoencoder (VAE). This separation enhances the model’s capacity to concentrate on dynamic trajectories while effectively reconstructing static scenes. The efficacy of Occ-LLM has been validated across key tasks, including 4D occupancy forecasting, self-ego planning, and occupancy-based scene question answering. Comprehensive evaluations demonstrate that Occ-LLM significantly surpasses existing state-of-the-art methodologies, achieving gains of about 6% in Intersection over Union (IoU) and 4% in mean Intersection over Union (mIoU) for the task of 4D occupancy forecasting. These findings highlight the transformative potential of Occ-LLM in reshaping current paradigms within robotic and autonomous driving.

I. INTRODUCTION

Large Language Models (LLMs) have evolved rapidly [1], [47], [42], [53], becoming integral to advancing artificial intelligence across various industries [32], [33], [21], [13]. Initially designed for natural language processing, LLMs have demonstrated remarkable adaptability in complex domains such as autonomous driving due to their robust generalization capabilities [5], [16], [10], [39]. These capabilities are particularly essential for robotic or autonomous driving systems, which currently lack generalization [6], [9]. Currently, LLM applications in autonomous driving mainly use image-based inputs [22], which lack the spatial perception needed for comprehensive environmental understanding. Existing methods in vision-based [39], [16] and LiDAR-based [41], [38] approaches, while enhancing vehicle navigation and environmental understanding, are computationally intensive and often lack transparency in intermediate reasoning processes.

Occupancy serves as a highly expressive modality in autonomous driving [29], offering rich spatial and semantic insights by comprehensively representing both the foreground and background of a scene. This universal representation

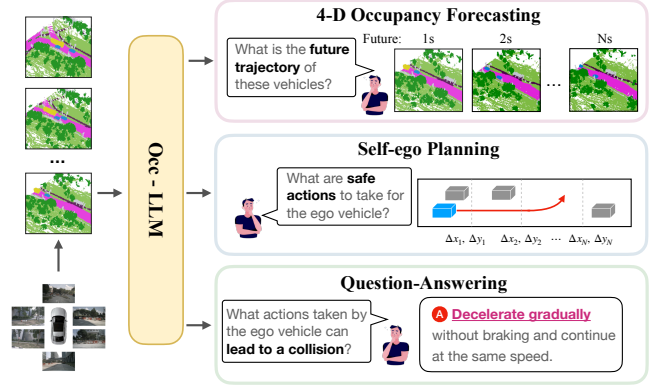


Fig. 1. We present Occ-LLM, an occupancy-based large language model designed for autonomous driving scene prediction, planning, and understanding (zoom in for the best view).

facilitates the perception of objects regardless of their specific categories, whether known or unidentified. Notably, leading automotive manufacturers, such as Tesla [43], are progressively adopting occupancy-based systems within their vehicles, highlighting a shift towards this robust method of environmental interpretation.

This paper aims to develop a foundational model for various downstream tasks in autonomous driving by leveraging the sophisticated analytical and generalization capabilities of LLMs to interpret and utilize occupancy grids. However, direct integration of occupancy representation into LLMs is challenging due to the unbalanced occupancy categories and the predominance of voxels representing air, leading to inefficient learning and memory issues. To overcome these challenges, we propose a novel method termed the Motion Separation Variational Autoencoder (MS-VAE). This approach separates voxels associated with movable entities (e.g., cars, pedestrians) from those related to immovable structures (e.g., streets, greenery) within the occupancy scene. By doing so, it enhances the model’s focus on dynamic object trajectories and improves the reconstruction of static scenes, akin to residual learning. This separation significantly reduces learning difficulties and improves overall model performance.

Our occupancy-based large language model (Occ-LLM) is meticulously designed to cater to a diverse range of applications within the domain of autonomous driving. Principal applications of our model include 4D occupancy scene forecasting, self-ego planning, and occupancy-based scene question answering (QA), as shown in Fig. 1. These appli-

¹Tianshuo Xu, Hao Lu, and Yingcong Chen are with the department of AI Thrust, Information Hub of Hong Kong University of Science and Technology (Guangzhou). txu647@connect.hkust-gz.edu.cn, hlu585@connect.hkust-gz.edu.cn, yingcongchen@ust.hk

²Xu Yan, Yingjie Cai, and Bingbing Liu are with the Huawei Noah’s Ark Lab. yanxu44@huawei.com, caiyingjie@link.cuhk.edu.hk liu.bingbing@huawei.com

*The corresponding author.

cations are integral to augmenting the safety, efficiency, and reliability of autonomous driving systems. To validate the effectiveness of our models, we conducted extensive evaluations comparing Occ-LLM to other state-of-the-art methods. Our model demonstrated superior performance, achieving a 32.52% IoU and a 20.99% mIoU in 4-D occupancy scene forecasting, significantly outperforming the state-of-the-art model, which achieved an IoU of 26.63% and an mIoU of 17.14% (the average over 3-second). For self-ego planning, our model reduced the 3-second average L2 distance to 0.28 meters, compared to the 1.17 meters achieved by the leading alternative. Additionally, in occupancy-based scene QA, Occ-LLM consistently provided accurate and reliable responses, thereby enhancing the decision-making capabilities in autonomous driving system.

The main contributions of this paper are listed below:

- We introduce an occupancy-based large language model (Occ-LLM) for autonomous driving, demonstrating superior scene comprehension.
- We propose the Motion Separation Variational Autoencoder (MS-VAE), which manages large volumes of occupancy grid data by distinguishing between movable and immovable elements, enhancing system performance across various indicators
- We showcase the versatility of Occ-LLM through its applications in 4D occupancy scene forecasting, self-ego planning, and occupancy-based scene question answering, illustrating its superiority across multiple dimensions of autonomous driving.
- We showcase the generalization capabilities of Occ-LLM by accessing existing occupancy prediction methods, illustrating its practicability for autonomous driving.

II. RELATED WORK

A. Multimodal Large Language Model

Recent advancements in Multimodal Large Language Models (MLLMs) have sparked interest by combining the advanced reasoning capabilities of LLMs with image, video, and audio data [24], [56], [27], [28]. These models have shown remarkable proficiency in tasks such as zero-shot and few-shot image classification, segmentation, and object detection by leveraging the synergy between visual and textual data. In the context of autonomous driving, LLMs address a critical gap by enhancing scene understanding, providing richer semantic context, and facilitating decision-making processes, which current systems lack. Several methods have been proposed to leverage LLMs in autonomous driving. Vision-based approaches, such as DriveGPT4, interpret video inputs to generate driving-related textual responses [5], while models like HiLM-D enhance hazard identification and intention prediction through high-resolution visual data [11]. Lidar-based methods utilize vectorized visual embeddings to equip LLMs with environmental perception capabilities, enabling detailed analysis of the driving scene [15].

B. Occupancy

Recently, 3D semantic occupancy provides a more detailed representation of the environment by explicitly modeling the occupancy status of each voxel within a 3D grid. SSCNet [40] was the first to introduce the task of semantic scene completion, integrating geometric and semantic information. Subsequent works commonly utilize geometric inputs with explicit depth information [35], [23], [51], [7]. MonoScene [4] proposed the first monocular approach for semantic scene completion, using a 3D UNet [36] to process voxel features generated through sight projection. Various networks based on the transfer architecture have been designed [20], [20], [54]. Additionally, several concurrent works have focused on proposing surrounding-view benchmarks for 3D semantic occupancy prediction, contributing to the rapid advancement of the occupancy community [49], [49], [50], [45], [44]. OccWorld learns a world model based on 3D occupancy, which has attracted much attention with its interpretability and efficiency. Further, this paper attempts to use the large language model as a bridge to unify occupancy tasks.

III. METHODS

This section introduces the Occ-LLM framework, which integrates Large Language Models (LLMs) with occupancy representation to improve autonomous driving systems (Fig. 2). The framework enhances spatial and semantic understanding, aiding scene interpretation and decision-making. We first convert multiview images into occupancy representation using existing methods. In Sec. III-A, we present the core Motion Separation Variational Autoencoder (MS-VAE), which differentiates between dynamic and static elements, reducing computational load and improving learning efficiency. The MS-VAE output is further processed and flattened for input into the LLM (Sec. III-B). Designed for various autonomous driving tasks, the Occ-LLM supports 4D occupancy forecasting, self-ego planning, and occupancy-based scene question answering (Sec. III-C), enhancing safety and effectiveness.

A. Motion Separation Variational Autoencoder

Building on established multi-modal LLM integration methods [27], [16], [37], we aim to train a Variational Autoencoder (VAE) to facilitate modal fusion and reduce computational costs. Direct integration of occupancy representation into LLMs faces challenges due to unbalanced occupancy categories and the predominance of air voxels, resulting in sparse and inefficient data representations. To overcome this, we propose the Motion Separation Variational Autoencoder (MS-VAE), which separates dynamic and static components within the occupancy grid. This enhances encoding efficiency and shifts focus to dynamic elements essential for autonomous navigation. MS-VAE thus enables more balanced and effective integration into LLM frameworks.

The core concept of the Motion Separation Variational Autoencoder (MS-VAE) involves training two distinct VQ-VAEs to encode and decode moving and static occupancy voxels separately. However, we discovered that maintaining

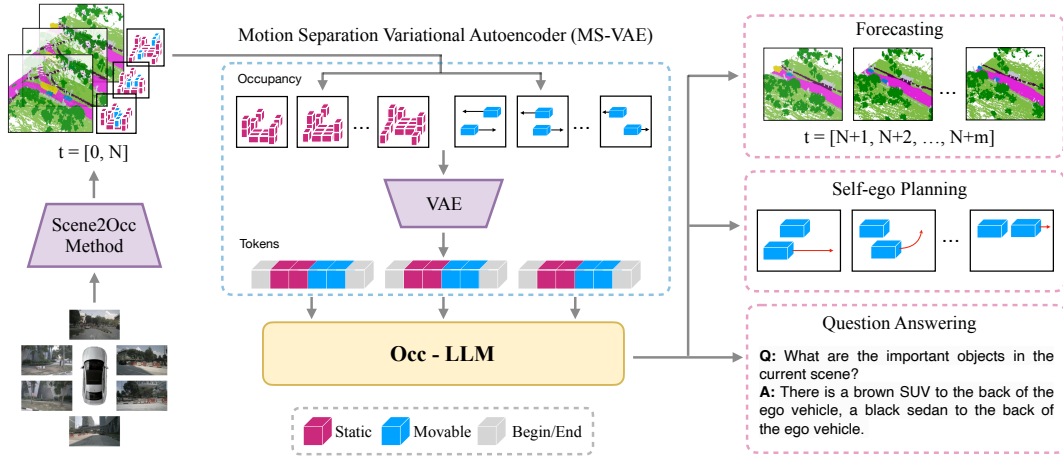


Fig. 2. Overview of the proposed Occ-LLM framework. Initially, results from multiview cameras are converted into occupancy representations utilizing existing occupancy prediction algorithms. Subsequently, the Motion Separation strategy is employed to differentiate voxels associated with moving objects from static elements. These differentiated voxels are then independently encoded into latent representations using our custom-designed VAE. Finally, these latents are processed as specified in Section III-B before being integrated into the LLM, completing the preparatory steps for downstream applications.

a single encoder and decoder while utilizing two different codebooks for moving and static voxels can also yield satisfactory results. For clarity, we describe this approach mathematically.

Let \mathbf{x} represent the input occupancy representation, with \mathbf{x}_m and \mathbf{x}_s denoting the moving and static voxels, respectively. The encoder $q_\phi(z|\mathbf{x})$ maps the input \mathbf{x} to a latent space \mathbf{z} . For the MS-VAE, we define two separate latent variables \mathbf{z}_m and \mathbf{z}_s for moving and static voxels:

$$\mathbf{z}_m \sim q_\phi(\mathbf{z}_m|\mathbf{x}_m), \quad \mathbf{z}_s \sim q_\phi(\mathbf{z}_s|\mathbf{x}_s). \quad (1)$$

Each encoded latent \mathbf{z}_m and \mathbf{z}_s searches in the corresponding codebook \mathbf{C}_m and \mathbf{C}_s , and is replaced by the most similar codebook entry before being input to the decoder. This process is represented as:

$$\mathbf{z}'_m = \operatorname{argmin}_{\mathbf{c}_m \in \mathbf{C}_m} \|\mathbf{z}_m - \mathbf{c}_m\|, \quad \mathbf{z}'_s = \operatorname{argmin}_{\mathbf{c}_s \in \mathbf{C}_s} \|\mathbf{z}_s - \mathbf{c}_s\|. \quad (2)$$

The decoder $p_\theta(\mathbf{x}|\mathbf{z})$ reconstructs the input from the quantized latent variables \mathbf{z}'_m and \mathbf{z}'_s :

$$\hat{\mathbf{x}}_m = p_\theta(\mathbf{x}_m|\mathbf{z}'_m), \quad \hat{\mathbf{x}}_s = p_\theta(\mathbf{x}_s|\mathbf{z}'_s). \quad (3)$$

To facilitate the separation of motion and static elements within the occupancy representation, we apply transformations based on the classification of voxels. Let \mathcal{M} denote the set of movable classes. We define indicator functions for motion and air-filling in the modified occupancy representation as follows:

Define an indicator function $\mathbf{1}_{\mathcal{M}}(\mathbf{x})$ such that:

$$\mathbf{1}_{\mathcal{M}}(\mathbf{x}) = \begin{cases} 1 & \text{if } \mathbf{x} \in \mathcal{M}, \\ 0 & \text{otherwise.} \end{cases} \quad (4)$$

The modified motion occupancy \mathbf{x}'_m and static occupancy \mathbf{x}'_s are then given by:

$$\mathbf{x}'_m = (1 - \mathbf{1}_{\mathcal{M}}(\mathbf{x})) \cdot \mathbf{x}_m, \quad (5)$$

$$\mathbf{x}'_s = \mathbf{1}_{\mathcal{M}}(\mathbf{x}) \cdot \text{air} + (1 - \mathbf{1}_{\mathcal{M}}(\mathbf{x})) \cdot \mathbf{x}_s, \quad (6)$$

where air denotes the representation of air in the static occupancy grid, typically encoded as a placeholder value that represents unoccupied space.

To reconstruct the raw occupancy representation, we utilize a mask $= (\hat{\mathbf{x}}_m \neq 0)$ to differentiate active motion regions. The reconstructed occupancy $\hat{\mathbf{x}}$ combines the static and motion components as follows:

$$\hat{\mathbf{x}} = \hat{\mathbf{x}}_m \cdot \text{mask} + \hat{\mathbf{x}}_s \cdot (1 - \text{mask}). \quad (7)$$

The overall loss function for training the MS-VAE combines the reconstruction loss and the commitment loss to ensure the encoded latent is close to the codebook entries:

$$\mathcal{L} = \mathbb{E}_{q_\phi(\mathbf{z}_m|\mathbf{x}_m)} [\log p_\theta(\mathbf{x}_m|\mathbf{z}'_m)] + \mathbb{E}_{q_\phi(\mathbf{z}_s|\mathbf{x}_s)} [\log p_\theta(\mathbf{x}_s|\mathbf{z}'_s)] + \beta (\|\mathbf{z}_m - \mathbf{z}'_m\|^2 + \|\mathbf{z}_s - \mathbf{z}'_s\|^2). \quad (8)$$

By leveraging separate codebooks for the moving and static voxels while keeping a unified encoder and decoder, and by appropriately handling the occupancy representation, the MS-VAE effectively captures the distinct characteristics of each voxel type, resulting in improved occupancy reconstruction and generalization.

In addition, the overall VAE architecture referred to the methodology outlined in OccWorld's implementation [55], specifically treating the occupancy as 2D data with 16 channels and employing a 2D VAE for encoding and decoding. However, to preserve the integrity of three-dimensional information, we integrate a layer of lightweight 3D convolution both prior to the Encoder and after the Decoder. This modification respects the spatial dimensions inherent to the occupancy representation and substantially enhances the reconstructed occupancy's quality. This approach, in contrast to the conventional usage of a 2D VAE, significantly improves the fidelity of the occupancy representation in three-dimensional space.

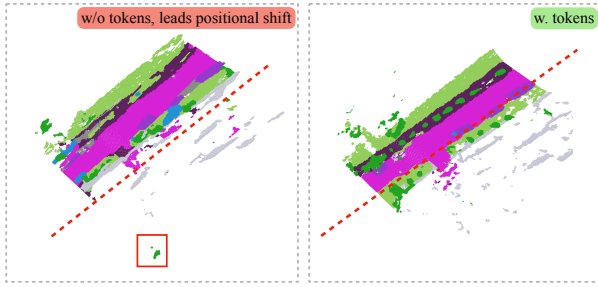


Fig. 3. Illustration of the positional shift problem in occupancy representation, where the red dotted line represents the central axis, and the red box signifies the occurrence of an object in the subsequent frame that appears within the current frame. This problem is mitigated by appending tokens to the beginning `<occ>` and end `</occ>` of each frame’s latent occupancy representation.

B. Pre-processing of Integrating Occupancy with LLM

Patchify. Following the encoding of raw occupancy representation using the MS-VAE, the resulting latent representation remains substantial. To address this, we adopt an approach akin to the Vision Transformer (ViT) [12] by partitioning the occupancy latent space into small grids and flattening it. Our observations indicate that the patch size significantly impacts the quality of occupancy reconstruction. This is because predicting future occupancy frames encompasses aspects of perception and low-level vision tasks. For instance, perception tasks typically benefit from larger patch sizes, facilitating a better understanding of the semantic information of the input data [12]. Conversely, low-level vision tasks often employ smaller patch sizes to achieve higher-quality data reconstruction [2]. Through an ablation study, we determined that a patch size of 10 yields optimal results.

Frame separation. We found that the flattened occupancy latent for each frame is relatively long, and directly concatenating the flattened occupancy latent of multiple frames leads to positional drift in the generated occupancy. This drift manifests as portions of occupancy from one frame appearing in subsequent frames, causing a cascading misalignment (shown in Fig. 3).

To address this issue, we propose a straightforward but effective solution: adding specific text tokens at the beginning and end of each occupancy latent frame. Specifically, we use `<occ>` at the beginning and `</occ>` at the end. These tokens delineate the intervals between frames during inference, effectively eliminating the drift problem.

Pre-fusion. We introduce a pre-fusion method to better establish the connection between occupancy representation and self-ego actions. This method involves first encoding self-ego actions through multiple MLP layers. Similar to the approach SE-Net [17], we then use the encoded action latent as a weight to modulate the occupancy tents. This technique enhances the consistency between the occupancy representation and the self-ego actions, improving overall model performance.

C. Downstream Tasks

The Occ-LLM framework supports a variety of downstream tasks critical for enhancing autonomous driving systems, including 4D occupancy forecasting, self-ego planning, and occupancy-based scene question answering. Task switching is managed through specific prompts: `<<4-D occupancy forecasting and self-ego planning>>` initiates the combined task of 4D occupancy forecasting and self-ego planning, while `<<question-answering>>` triggers the question-answering task. These tasks collectively enhance situational awareness and decision-making. 4-D occupancy forecasting predicts environmental dynamics, which is crucial for anticipating hazards. Self-ego planning uses these forecasts for safe, efficient navigation. Occupancy-based scene question answering interprets complex situations, aiding in informed decision-making. Together, these capabilities significantly improve autonomous driving systems’ safety, reliability, and efficiency.

IV. EXPERIMENTS

In this section, we present an extensive set of experiments to evaluate the performance of our proposed Occ-LLM. We utilize Llama2 [47] as the foundational model. We evaluate 4D occupancy forecasting using Intersection over Union (IoU) [14] and mean Intersection over Union (mIoU) [8] metrics. Self-ego planning capability is assessed using the L2 distance metric.

We employ the Nuscenes dataset [3], which comprises 1000 scenes. These scenes are divided into 700 for training, 150 for validation, and 150 for testing. Each scene contains approximately 50 frames, corresponding to an occupancy scene. The occupancy representation has dimensions of (200,200,16), where the first (200,200) represents the length and width, and 16 represents the height. This dataset configuration enables a comprehensive assessment and validation of our model’s performance across various scenarios.

A. Comparisons with the State-of-the-art Methods

1) *4-D occupancy forecasting and self-ego planning:* Table I compares our methods with state-of-the-art approaches in 4D occupancy forecasting and motion planning, providing metrics such as IoU, mIoU, and L2 distance at 1, 2, and 3-second intervals. Our methods consistently outperform the state-of-the-art in accuracy and consistency, as shown in Fig. 4.

The evaluated methods include LiDAR-based approaches like IL [34], NMP [52], and FF [18], as well as camera-based methods such as UniAD [19], VAD-Base [22], and OccNet [46]. We also integrate predicted occupancy data into our Occ-LLM framework, achieving higher performance with models like BevFormer+Ours, which reaches an average IoU of 23.79%, mIoU of 10.21%, and an L2 distance of 0.43 meters.

Compared to occupancy-based methods, our approach surpasses OccWorld, with an average IoU of 32.52%, mIoU of 20.99%, and an L2 distance of 0.28 meters, demonstrating superior accuracy and reliability for autonomous driving.

TABLE I

QUANTITATIVE RESULTS OF 4D OCCUPANCY FORECASTING AND MOTION PLANNING. “VANILLA” REFERS TO THE DIRECT FLATTENING OF OCCUPANCY REPRESENTATION AND ITS INJECTION INTO THE LLM FOR TRAINING.

Methods	Input	IoU \uparrow (%)				mIoU \uparrow (%)				L2 \downarrow (m)			
		1s	2s	3s	Avg.	1s	2s	3s	Avg.	1s	2s	3s	Avg.
IL	LiDAR	-	-	-	-	-	-	-	-	0.44	1.15	2.47	1.35
NMP	LiDAR	-	-	-	-	-	-	-	-	0.53	1.25	2.67	1.48
FF	LiDAR	-	-	-	-	-	-	-	-	0.55	1.20	2.78	1.43
UniAD	Camera	-	-	-	-	-	-	-	-	0.48	0.96	1.65	1.03
VAD-Base	Camera	-	-	-	-	-	-	-	-	0.54	1.15	1.98	1.22
OccNet	Camera	-	-	-	-	-	-	-	-	1.29	2.13	2.99	2.14
OccWorld-S	Camera	21.09	16.17	4.95	5.00	0.28	0.26	0.24	0.26	0.67	1.69	3.13	1.83
BevFormer+OccWorld	Camera	23.28	17.71	14.06	18.35	5.04	3.34	1.24	3.20	0.43	0.87	1.31	0.87
BevDet+OccWorld	Camera	24.12	18.19	15.44	19.25	6.21	4.01	1.39	3.87	0.41	0.84	1.28	0.84
FBOCC+OccWorld	Camera	24.22	18.49	15.64	19.45	6.55	4.24	1.44	4.07	0.37	0.77	1.14	0.76
BevFormer+Ours	Camera	25.35	21.09	16.17	20.87	9.11	7.98	5.02	7.37	0.26	0.67	0.98	0.64
BevDet+Ours	Camera	27.07	23.42	18.56	23.02	10.99	9.92	8.78	9.90	0.23	0.48	0.74	0.48
FBOCC+Ours	Camera	27.11	24.07	20.19	23.79	11.28	10.21	9.13	10.21	0.21	0.40	0.67	0.43
<i>Vanilla</i>	Occ.	21.36	18.31	14.82	18.16	14.15	9.80	6.77	10.24	0.48	0.62	0.79	0.63
OccNet	Occ.	-	-	-	-	-	-	-	-	1.29	2.31	2.98	2.25
OccWorld	Occ.	34.63	25.07	20.18	26.63	25.78	15.14	10.51	17.14	0.43	1.08	1.99	1.17
Ours	Occ.	36.65	32.14	28.77	32.52	24.02	21.65	17.29	20.99	0.12	0.24	0.49	0.28

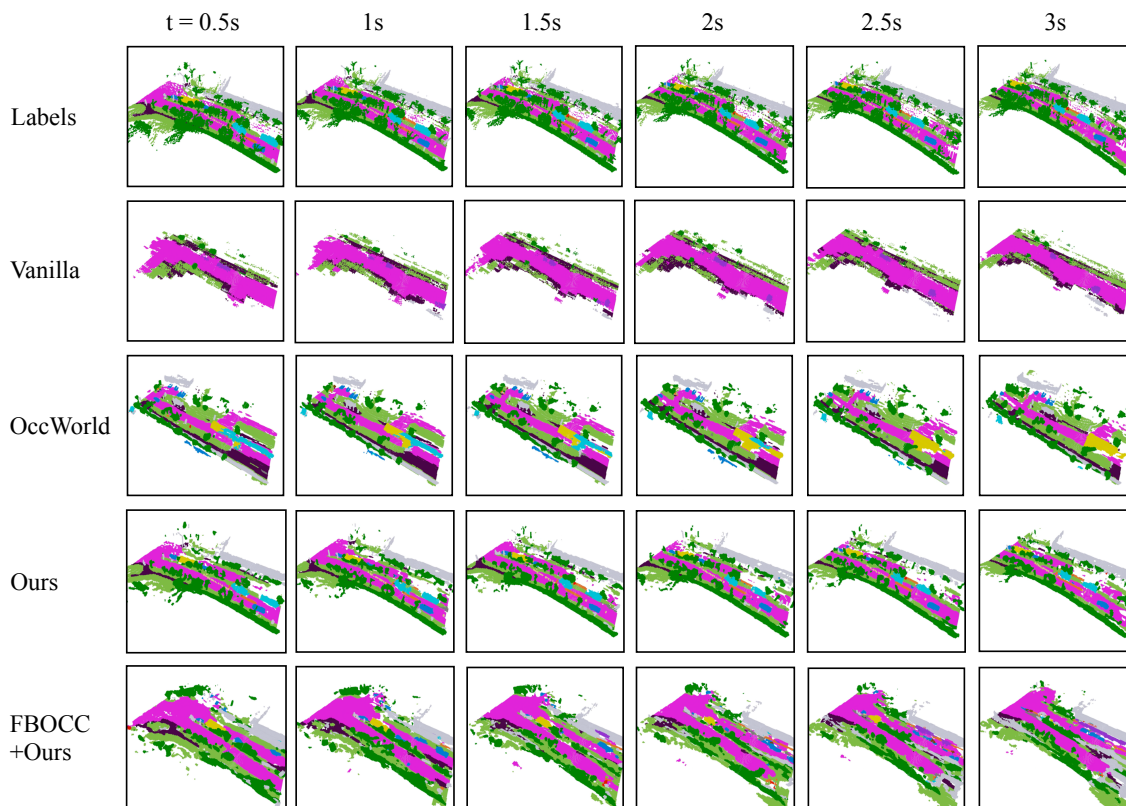


Fig. 4. Qualitative 4-D occupancy forecasting results of our Occ-LLM. “Vanilla” refers to the direct flattening of occupancy representation and its injection into the LLM for training (**zoom in for the best view**).

2) *Question-answering*: Our proposed method demonstrates advanced question-answering capabilities specifically tailored for autonomous driving scenarios. As illustrated in Figure 5, the system effectively interprets multi-view camera inputs to predict occupancy and provide accurate responses to queries regarding the driving environment. It can identify critical objects in the scene, recommend safe maneuvers for the ego vehicle, and describe potential hazards, such as pedestrians preparing to cross the road.

To quantitatively assess our system’s performance, we

conducted a comparative evaluation against the DriveLM model [39] using standard metrics, namely BLEU [31], ROUGE.L [26], CIDEr [48], and GPT Score [30], as presented in Table II. Details of these evaluation metrics are provided in [39]. Our model outperforms DriveLM across all metrics, achieving superior scores. These results substantiate the effectiveness of our approach in delivering accurate and contextually relevant answers within autonomous driving environments.

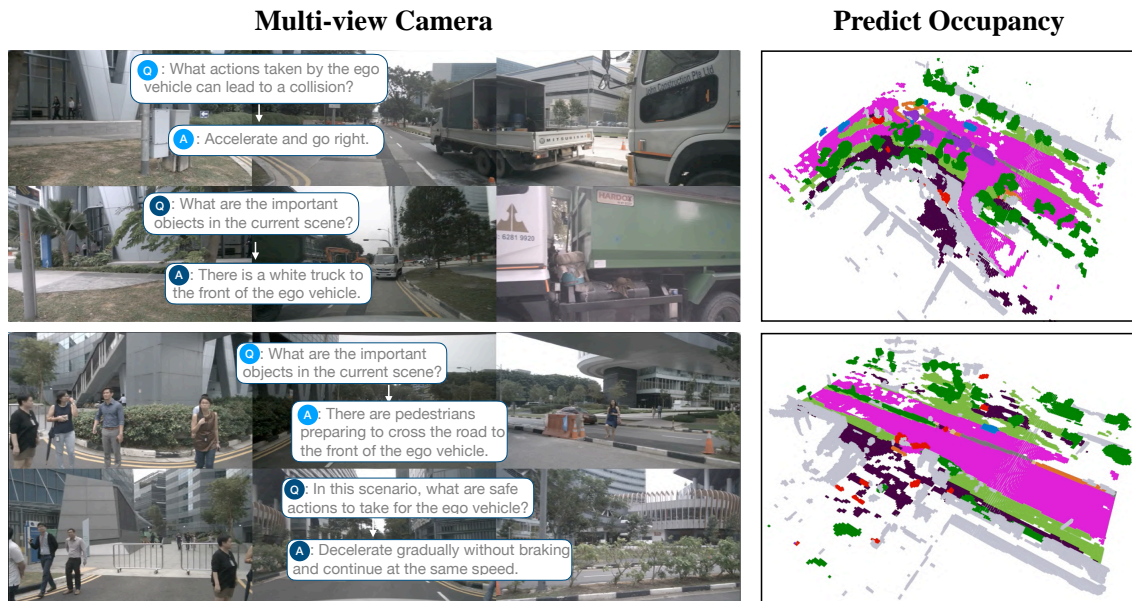


Fig. 5. Qualitative question-answering results of our Occ-LLM. The left panel displays the raw scene data, while the right panel shows the predicted occupancy generated by FBOCC [25]. The questions (Q) and the corresponding predicted answers (A) are illustrated (zoom in for the best view).

TABLE II

QUANTITATIVE EVALUATION OF QUESTION-ANSWERING PERFORMANCE METRICS COMPARING OUR OCC-LLM WITH DRIVELM.

Methods	Bleu	ROUGE.L	CIDEr	GPT Score \uparrow
DriveLM	0.68	0.74	0.32	52.91
Ours	0.71	0.75	2.95	56.72

TABLE III

COMPARATIVE ANALYSIS OF OCCWORLD'S VAE [55] AND THE PROPOSED MS-VAE. THE BASELINE MODEL EMPLOYS THE SAME ARCHITECTURE AS OCCWORLD'S VAE.

Methods	Latent Shape	Parameters(M)	Reconstruction	
			IoU \uparrow	mIoU \uparrow
OccWorld	50,50,128	14.28	59.07	60.50
Baseline	50,50,32	2.25	57.90	59.34
+3D Conv.	50,50,32	2.30	61.94	65.81
+Motion Separation	50,50,64	2.30	62.74	71.08

B. Ablation Study

1) *Comparative analysis of OccWorld's VAE and the proposed MS-VAE:* Table III compares OccWorld's VAE [55] with our proposed MS-VAE, showing significant improvements in reconstruction performance. The addition of 3D convolution layers and the Motion Separation strategy has increased IoU and mIoU, with MS-VAE achieving 62.74% IoU and 71.08% mIoU, compared to 59.07% and 60.50% for OccWorld's VAE.

2) *Comparative analysis of different patch sizes in patchify:* Table IV examines the effect of varying patch sizes on reconstruction performance. A patch size of 10 performs best, with an IoU of 32.48% and mIoU of 26.16% on the Trainset, and 27.12% and 26.83% on the Valset, balancing detail capture and efficiency.

3) *Ablation study of Occ-LLM modules:* Table V shows an ablation study of Occ-LLM modules. The baseline achieves

TABLE IV

COMPARATIVE ANALYSIS OF DIFFERENT PATCH SIZES IN PATCHIFY. EACH VALUE REPRESENTS THE AVERAGE OVER A 3-SECOND INTERVAL.

Patch size	Trainset		Valset	
	IoU \uparrow	mIoU \uparrow	IoU \uparrow	mIoU \uparrow
1	20.91	15.14	16.46	7.71
5	28.94	22.61	26.55	25.81
10	32.48	26.16	27.12	26.83
25	25.97	19.69	16.33	11.89

TABLE V

ABLATION STUDY OF OCC-LLM MODULES. EACH VALUE REPRESENTS THE PERFORMANCE ON THE VALIDATION SET.

Modules	Valset		
	IoU \uparrow (%)	mIoU \uparrow (%)	L2 \downarrow (m)
Baseline	20.67	16.63	0.82
+Pre Fusion	24.44	18.27	0.69
+Motion Separation	32.52	20.99	0.28

20.67% IoU, 16.63% mIoU, and 0.82m L2 distance. Adding the Pre Fusion module improves these metrics, and incorporating the Motion Separation (MS) module further boosts IoU to 32.52%, mIoU to 20.99%, and reduces L2 distance to 0.28m, highlighting the benefits of the MS module.

V. CONCLUSION

This paper introduces the Occupancy-based Large Language Model (Occ-LLM), which enhances autonomous driving by integrating LLMs with occupancy representation. It proposes the Motion Separation Variational Autoencoder (MS-VAE) to address category imbalance by separating dynamic objects from static scenes. Occ-LLM outperforms state-of-the-art methods in 4D occupancy forecasting, self-ego planning, and scene question answering, achieving higher Intersection over Union (IoU) and mean IoU (mIoU) scores and reducing planning errors.

REFERENCES

- [1] J. Achiam, S. Adler, S. Agarwal, L. Ahmad, I. Akkaya, F. L. Aleman, D. Almeida, J. Altenschmidt, S. Altman, S. Anadkat, et al. Gpt-4 technical report. *arXiv preprint arXiv:2303.08774*, 2023.
- [2] F. Bao, S. Nie, K. Xue, Y. Cao, C. Li, H. Su, and J. Zhu. All are worth words: A vit backbone for diffusion models. In *Proceedings of the IEEE/CVF Conference on Computer Vision and Pattern Recognition*, pages 22669–22679, 2023.
- [3] H. Caesar, V. Bankiti, A. H. Lang, S. Vora, V. E. Liong, Q. Xu, A. Krishnan, Y. Pan, G. Baldan, and O. Beijbom. nuscenes: A multimodal dataset for autonomous driving. In *CVPR*, pages 11621–11631, 2020.
- [4] A.-Q. Cao and R. de Charette. Monoscene: Monocular 3d semantic scene completion. In *CVPR*, pages 3991–4001, 2022.
- [5] L. Chen, O. Sinavski, J. Hünermann, A. Karnsund, A. J. Willmott, D. Birch, D. Maund, and J. Shotton. Driving with llms: Fusing object-level vector modality for explainable autonomous driving. *arXiv preprint arXiv:2310.01957*, 2023.
- [6] L. Chen, P. Wu, K. Chitta, B. Jaeger, A. Geiger, and H. Li. End-to-end autonomous driving: Challenges and frontiers. *arXiv preprint arXiv:2306.16927*, 2023.
- [7] X. Chen, K.-Y. Lin, C. Qian, G. Zeng, and H. Li. 3d sketch-aware semantic scene completion via semi-supervised structure prior. In *CVPR*, pages 4193–4202, 2020.
- [8] T. Cheng et al. Multiscale iou: A metric for evaluation of salient object detection with fine structures. *arXiv preprint arXiv:2105.14572*, 2021.
- [9] P. S. Chib and P. Singh. Recent advancements in end-to-end autonomous driving using deep learning: A survey. *IEEE Transactions on Intelligent Vehicles*, 2023.
- [10] V. Dewangan, T. Choudhary, S. Chandhok, S. Priyadarshan, A. Jain, A. K. Singh, S. Srivastava, K. M. Jatavallabhula, and K. M. Krishna. Talk2bev: Language-enhanced bird’s-eye view maps for autonomous driving. *arXiv preprint arXiv:2310.02251*, 2023.
- [11] X. Ding et al. Hilm-d: Towards high-resolution hazard identification and intention prediction for autonomous driving. *arXiv preprint arXiv:2310.02933*, 2023.
- [12] A. Dosovitskiy, L. Beyer, A. Kolesnikov, D. Weissenborn, X. Zhai, T. Unterthiner, M. Dehghani, M. Minderer, G. Heigold, S. Gelly, et al. An image is worth 16x16 words: Transformers for image recognition at scale. *arXiv preprint arXiv:2010.11929*, 2020.
- [13] J. Drápal, H. Westermann, and J. Savelka. Using large language models to support thematic analysis in empirical legal studies. *arXiv preprint arXiv:2310.18729*, 2023.
- [14] M. Everingham, L. Van Gool, C. K. Williams, J. Winn, and A. Zisserman. The pascal visual object classes (voc) challenge. *International Journal of Computer Vision*, 88(2):303–338, 2010.
- [15] K. Fu et al. Driving with vision-language models: Enhancing autonomous vehicles with multimodal ai. *arXiv preprint arXiv:2310.03021*, 2023.
- [16] A. Hu, L. Russell, H. Yeo, Z. Murez, G. Fedoseev, A. Kendall, J. Shotton, and G. Corrado. Gaia-1: A generative world model for autonomous driving. *arXiv preprint arXiv:2309.17080*, 2023.
- [17] J. Hu, L. Shen, and G. Sun. Squeeze-and-excitation networks. In *Proceedings of the IEEE conference on computer vision and pattern recognition*, pages 7132–7141, 2018.
- [18] P. Hu, A. Huang, J. Dolan, D. Held, and D. Ramanan. Safe local motion planning with self-supervised freespace forecasting. In *Proceedings of the IEEE/CVF Conference on Computer Vision and Pattern Recognition*, pages 12732–12741, 2021.
- [19] Y. Hu, J. Yang, L. Chen, K. Li, C. Sima, X. Zhu, S. Chai, S. Du, T. Lin, W. Wang, L. Lu, X. Jia, Q. Liu, J. Dai, Y. Qiao, and H. Li. Planning-oriented autonomous driving. In *Proceedings of the IEEE/CVF Conference on Computer Vision and Pattern Recognition*, 2023.
- [20] Y. Huang, W. Zheng, Y. Zhang, J. Zhou, and J. Lu. Tri-perspective view for vision-based 3d semantic occupancy prediction. In *CVPR*, pages 9223–9232, 2023.
- [21] J. Irons, C. Mason, P. Cooper, S. Sidra, A. Reeson, and C. Paris. Exploring the impacts of chatgpt on future scientific work. 2023.
- [22] B. Jiang, S. Chen, Q. Xu, B. Liao, J. Chen, H. Zhou, Q. Zhang, W. Liu, C. Huang, and X. Wang. Vad: Vectorized scene representation for efficient autonomous driving. In *Proceedings of the IEEE/CVF International Conference on Computer Vision*, pages 8340–8350, 2023.
- [23] J. Li, K. Han, P. Wang, Y. Liu, and X. Yuan. Anisotropic convolutional networks for 3d semantic scene completion. In *CVPR*, pages 3351–3359, 2020.
- [24] J. Li, D. Li, S. Savarese, and S. Hoi. Blip-2: Bootstrapping language-image pre-training with frozen image encoders and large language models. *arXiv preprint arXiv:2301.12597*, 2023.
- [25] Z. Li, Z. Yu, D. Austin, M. Fang, S. Lan, J. Kautz, and J. M. Alvarez. Fb-occ: 3d occupancy prediction based on forward-backward view transformation. *arXiv preprint arXiv:2307.01492*, 2023.
- [26] C.-Y. Lin. ROUGE: A package for automatic evaluation of summaries. In *Text Summarization Branches Out: Proceedings of the ACL-04 Workshop*, pages 74–81. Association for Computational Linguistics, 2004.
- [27] H. Liu, C. Li, Q. Wu, and Y. J. Lee. Visual instruction tuning. *arXiv preprint arXiv:2304.08485*, 2023.
- [28] H. Lu, X. Niu, J. Wang, Y. Wang, Q. Hu, J. Tang, Y. Zhang, K. Yuan, B. Huang, Z. Yu, et al. Gpt as psychologist? preliminary evaluations for gpt-4v on visual affective computing. *2024 IEEE/CVF Conference on Computer Vision and Pattern Recognition (CVPR) workshop*, 2024.
- [29] L. Mescheder, M. Oechsle, M. Niemeyer, S. Nowozin, and A. Geiger. Occupancy networks: Learning 3d reconstruction in function space. In *Proceedings of the IEEE/CVF conference on computer vision and pattern recognition*, pages 4460–4470, 2019.
- [30] OpenAI. GPT-4 technical report. *arXiv preprint arXiv:2303.08774*, 2023.
- [31] K. Papineni, S. Roukos, T. Ward, and W.-J. Zhu. Bleu: a method for automatic evaluation of machine translation. In *Proceedings of the 40th annual meeting of the Association for Computational Linguistics*, pages 311–318, 2002.
- [32] C. Qin, A. Zhang, Z. Zhang, J. Chen, M. Yasunaga, and D. Yang. Is chatgpt a general-purpose natural language processing task solver? *arXiv preprint arXiv:2302.06476*, 2023.
- [33] A. Rao, J. Kim, M. Kamineni, M. Pang, W. Lie, and M. D. Succi. Evaluating chatgpt as an adjunct for radiologic decision-making. *MedRxiv*, pages 2023–02, 2023.
- [34] N. D. Ratliff, J. A. Bagnell, and M. A. Zinkevich. Maximum margin planning. In *Proceedings of the 23rd international conference on Machine learning*, pages 729–736, 2006.
- [35] L. Roldao, R. de Charette, and A. Verroust-Blondet. Lmscnet: Lightweight multiscale 3d semantic completion. In *3DV*, 2020.
- [36] O. Ronneberger, P. Fischer, and T. Brox. U-net: Convolutional networks for biomedical image segmentation. In *MICCAI*, pages 234–241. Springer, 2015.
- [37] Y. Shi, B. Paige, P. Torr, et al. Variational mixture-of-experts autoencoders for multi-modal deep generative models. *Advances in neural information processing systems*, 32, 2019.
- [38] S. Shubodh, M. Omama, H. Zaidi, U. S. Parihar, and M. Krishna. Lip-loc: Lidar image pretraining for cross-modal localization. In *Proceedings of the IEEE/CVF Winter Conference on Applications of Computer Vision*, pages 948–957, 2024.
- [39] C. Sima, K. Renz, K. Chitta, L. Chen, H. Zhang, C. Xie, P. Luo, A. Geiger, and H. Li. Drivelm: Driving with graph visual question answering. *arXiv preprint arXiv:2312.14150*, 2023.
- [40] S. Song, F. Yu, A. Zeng, A. X. Chang, M. Savva, and T. Funkhouser. Semantic scene completion from a single depth image. In *CVPR*, pages 1746–1754, 2017.
- [41] K. Tang, X. Cao, Z. Cao, T. Zhou, E. Li, A. Liu, S. Zou, C. Liu, S. Mei, E. Sizikova, et al. Thma: Tencent hd map ai system for creating hd map annotations. In *Proceedings of the AAAI Conference on Artificial Intelligence*, volume 37, pages 15585–15593, 2023.
- [42] G. Team, R. Anil, S. Borgeaud, Y. Wu, J.-B. Alayrac, J. Yu, R. Soricut, J. Schalkwyk, A. M. Dai, A. Hauth, et al. Gemini: a family of highly capable multimodal models. *arXiv preprint arXiv:2312.11805*, 2023.
- [43] Tesla. The future of driving: Autopilot and full self-driving capabilities. https://www.youtube.com/watch?v=ODSJsvid_SU&ab_channel=Tesla, 2022.
- [44] X. Tian, T. Jiang, L. Yun, Y. Wang, Y. Wang, and H. Zhao. Occ3d: A large-scale 3d occupancy prediction benchmark for autonomous driving. *arXiv preprint arXiv:2304.14365*, 2023.
- [45] W. Tong, C. Sima, T. Wang, L. Chen, S. Wu, H. Deng, Y. Gu, L. Lu, P. Luo, D. Lin, et al. Scene as occupancy. In *ICCV*, pages 8406–8415, 2023.
- [46] W. Tong, C. Sima, T. Wang, L. Chen, S. Wu, H. Deng, Y. Gu, L. Lu, P. Luo, D. Lin, et al. Scene as occupancy. In *Proceedings of the*

- IEEE/CVF International Conference on Computer Vision*, pages 8406–8415, 2023.
- [47] H. Touvron, L. Martin, K. Stone, P. Albert, A. Almahairi, Y. Babaei, N. Bashlykov, S. Batra, P. Bhargava, S. Bhosale, et al. Llama 2: Open foundation and fine-tuned chat models. *arXiv preprint arXiv:2307.09288*, 2023.
 - [48] R. Vedantam, C. L. Zitnick, and D. Parikh. CIDEr: Consensus-based image description evaluation. In *Proceedings of the IEEE Conference on Computer Vision and Pattern Recognition (CVPR)*, pages 4566–4575. IEEE, 2015.
 - [49] X. Wang, Z. Zhu, W. Xu, Y. Zhang, Y. Wei, X. Chi, Y. Ye, D. Du, J. Lu, and X. Wang. Openoccupancy: A large scale benchmark for surrounding semantic occupancy perception. In *ICCV*, pages 17850–17859, 2023.
 - [50] Y. Wei, L. Zhao, W. Zheng, Z. Zhu, J. Zhou, and J. Lu. Surroundocc: Multi-camera 3d occupancy prediction for autonomous driving. In *ICCV*, pages 21729–21740, 2023.
 - [51] X. Yan, J. Gao, J. Li, R. Zhang, Z. Li, R. Huang, and S. Cui. Sparse single sweep lidar point cloud segmentation via learning contextual shape priors from scene completion. In *AAAI*, volume 35, pages 3101–3109, 2021.
 - [52] W. Zeng, W. Luo, S. Suo, A. Sadat, B. Yang, S. Casas, and R. Urtasun. End-to-end interpretable neural motion planner. In *Proceedings of the IEEE/CVF Conference on Computer Vision and Pattern Recognition*, pages 8660–8669, 2019.
 - [53] W. Zeng, X. Ren, T. Su, H. Wang, Y. Liao, Z. Wang, X. Jiang, Z. Yang, K. Wang, X. Zhang, et al. Pangu- α : Large-scale autoregressive pretrained chinese language models with auto-parallel computation. *arXiv preprint arXiv:2104.12369*, 2021.
 - [54] Y. Zhang, Z. Zhu, and D. Du. Occformer: Dual-path transformer for vision-based 3d semantic occupancy prediction. In *ICCV*, pages 9433–9443, 2023.
 - [55] W. Zheng, W. Chen, Y. Huang, B. Zhang, Y. Duan, and J. Lu. Occworld: Learning a 3d occupancy world model for autonomous driving. *arXiv preprint arXiv:2311.16038*, 2023.
 - [56] D. Zhu, J. Chen, X. Shen, X. Li, and M. Elhoseiny. Minigt-4: Enhancing vision-language understanding with advanced large language models. *arXiv preprint arXiv:2304.10592*, 2023.